Direct Probe of the Bent and Linear Geometries of the Core-Excited Renner-Teller Pair States by Means of the Triple-Ion-Coincidence Momentum Imaging Technique

Y. Muramatsu,[1] K. Ueda,[1,*] N. Saito,[2] H. Chiba,[1] M. Lavollée,[3] A. Czasch,[4] T. Weber,[4] O. Jagutzki,[4] H. Schmidt-Böcking,[4] R. Moshammer,[5] U. Becker,[6] K. Kubozuka,[7] and I. Koyano[7]

[1]*Institute of Multidisciplinary Research for Advanced Materials, Tohoku University, Sendai 980-8577, Japan*
[2]*National Metrology Institute of Japan, AIST, Tsukuba 305-8568, Japan*
[3]*LURE, Bâtiment 209d, Centre Universitaire Paris-Sud, F-91898, Orsay Cedex, France*
[4]*Institut für Kernphsik, Universität Frankfurt, D-60486 Frankfurt, Germany*
[5]*Max-Planck-Institut für Kernphysik, D-67119 Heidelberg, Germany*
[6]*Fritz-Haber-Institut der Max-Planck-Gesellshaft, D-14195 Berlin, Germany*
[7]*Department of Material Science, Himeji Institute of Technology, Kamigori, Hyogo 678-1297, Japan*

(Received 4 June 2001; published 18 March 2002)

The doubly degenerate core-excited Π state of CO_2 splits into two due to static Renner-Teller effect. Using the triple-ion-coincidence momentum imaging technique and focusing on the dependence of the measured quantities on the polarization of the incident light, we have probed, directly and separately, the linear and bent geometries for the B_1 and A_1 Renner-Teller pair states, as a direct proof of the static Renner-Teller effect.

DOI: 10.1103/PhysRevLett.88.133002 PACS numbers: 33.20.Rm, 33.15.Bh, 33.20.Wr

Generally, when a core electron of a free molecule is excited to an unoccupied molecular orbital, Auger emission occurs and the molecular fragmentation follows. Within the lifetime of the order of femtoseconds, however, the nuclear motion proceeds in the core-excited state [1,2]. In the case of polyatomic molecules, nontotally symmetric nuclear motion may be caused via the transition from the ground to core-excited states because they may have different symmetries in stable geometry [3–5]. Nontotally symmetric nuclear motion is of particular interest because the excitation of it may open up a new dynamical pathway of molecular dissociation [6,7].

The change in symmetry of stable geometry between the ground and core-excited states is well understood with the help of the $(Z + 1)$ equivalent-core model in which a core-excited atom with nuclear charge Z is replaced by the $(Z + 1)$ atom. For example, the core-excited state of a linear molecule CO_2 with a C $1s$ electron promoted to the lowest unoccupied molecular orbital $2\pi_u$ is approximated by the ground state of the bent molecule NO_2 and thus the C $1s^{-1}2\pi_u$ state is also expected to be bent [8–11].

The structural change of the core-excited molecule, as well as of the core-excited solid crystal, can be generalized as a result of vibronic coupling of diabatic potential surfaces via nontotally symmetric nuclear motion [12–17]. For example, the doubly degenerate core-excited Π states of a linear molecule, such as C/O $1s^{-1}2\pi_u\ ^1\Pi_u$ in CO_2 concerned here, split into two states along the nontotally symmetric bending coordinate Q_2 due to vibronic coupling via the Q_2 mode, referred to as static Renner-Teller (RT) effect [8,10,11,18–20]. A schematic representation of the RT pair states split from C/O $1s^{-1}2\pi_u\ ^1\Pi_u$ is given in Fig. 1. The lower branch of the RT pair states has a stable bent geometry. This bent state has an electron in the π orbital that lies in the bending plane of the molecule (in-plane, A_1 in C_{2v}). The upper branch, on the other hand, remains linear. This linear state has an electron in the π orbital that lies perpendicularly to the bending plane (out-of-plane, B_1 in C_{2v}).

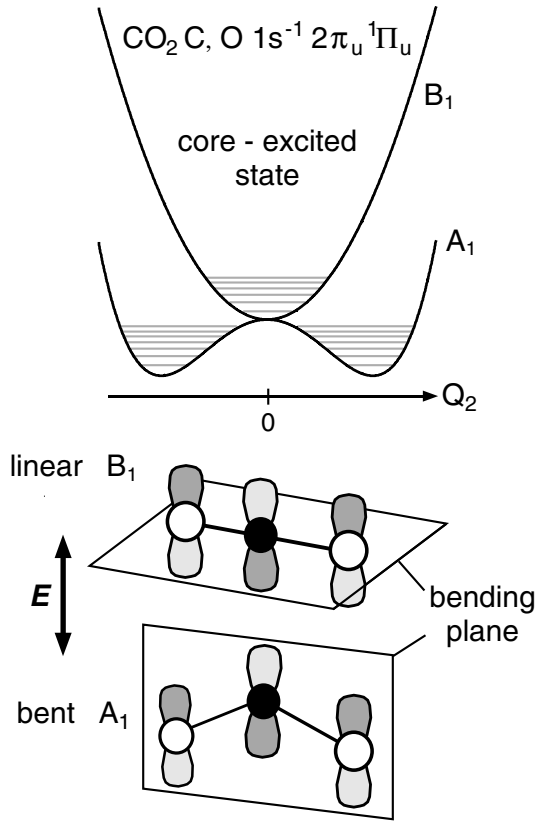

FIG. 1. A schematic representation of the Renner-Teller pair states split from C/O $1s^{-1}2\pi_u\ ^1\Pi_u$. The geometries of the $2\pi_u$ orbital and the bending planes of the A_1 and B_1 states are shown in the lower part.

In the present Letter we demonstrate that the bent and linear geometries of the core-excited RT pair states A_1 and B_1, which were not resolved in any previous work [8–11,19,20], can be probed, as a direct proof of the static RT effect. The key point here is that the bending motion proceeds in the direction parallel to the polarization vector E of the incident light in the A_1 state and perpendicular to E in the B_1 state. Thus one can probe the geometry of these two RT pair states separately if one can measure the bond angle by selecting the directions of the bending motions parallel and perpendicular to E.

The experimental technique we employ here is the triple-ion-coincidence momentum imaging. Using this technique we measure the linear momenta of the three ions C^+, O^+, and O^+ in coincidence. The triply charged molecular parent ion CO_2^{3+} is produced by the Auger decay of the inner-shell excited states of CO_2. This triply charged molecular ion has high internal energy and breaks up very rapidly due to the Coulomb explosion. The bond breaking is simultaneous and the axial-recoil approximation [21,22] is valid. Thus linear momenta of the fragment ions reflect the geometry of the molecule at the time when the Auger decay takes place. Then we can select the state in which the direction of the bending motion is parallel to the incident light polarization vector E or the state in which the molecular plane is perpendicular to the E vector, by examining the linear momenta of the three fragment ions C^+, O^+, and O^+. Vector correlation among the linear momenta of the three fragment ions thus measured separately for these two states give us the direct information about the geometries of these two states.

The experiments are carried out on the c branch of the soft x-ray photochemistry beam line 27SU at SPring-8 [23] and on the beam line SA22 at Super-ACO. A beam of the sample gas CO_2 is introduced into the ionization point and crossed with the photon beam. Three fragment ions C^+, O^+, and O^+ produced from a triply charged parent molecular ion CO_2^{3+} are detected in coincidence by means of a time-of-flight (TOF) mass spectrometer equipped with a multihit position-sensitive detector consisting of microchannel plates and a position-sensitive anode. The position-sensitive anode is homemade multianodes for the experiment at Super-ACO [24] and a delay-line anode (Roentdek DLD80) for the experiment at SPring-8. The position (x, y) and the arrival time t for each of the three ions (C^+, O^+, and O^+) measured in coincidence provide the linear momentum for each of the three ions. The TOF axis is fixed in the direction perpendicular to both the photon beam direction and E. The experiments are carried out both for the C 1s and O 1s excitations in CO_2. The photon energy band passes employed are ~30 meV for the C 1s excitation and ~55 meV for the O 1s excitation. The general results are surprisingly similar for the C 1s excitation and for the O 1s excitation. We thus exhibit the results for the O 1s excitation first in Fig. 2 and then discuss its comparison with the C 1s excitation in Fig. 3.

We focus on the vector correlation among the linear momenta of the three fragment ions produced in the three-body breakup $CO_2^{3+} \rightarrow C^+ + O^+ + O^+$. This correlation can be well represented by the Newton diagrams. In the Newton diagrams in Fig. 2, the amplitude of the linear momentum of the first O^+ is normalized to unity and the

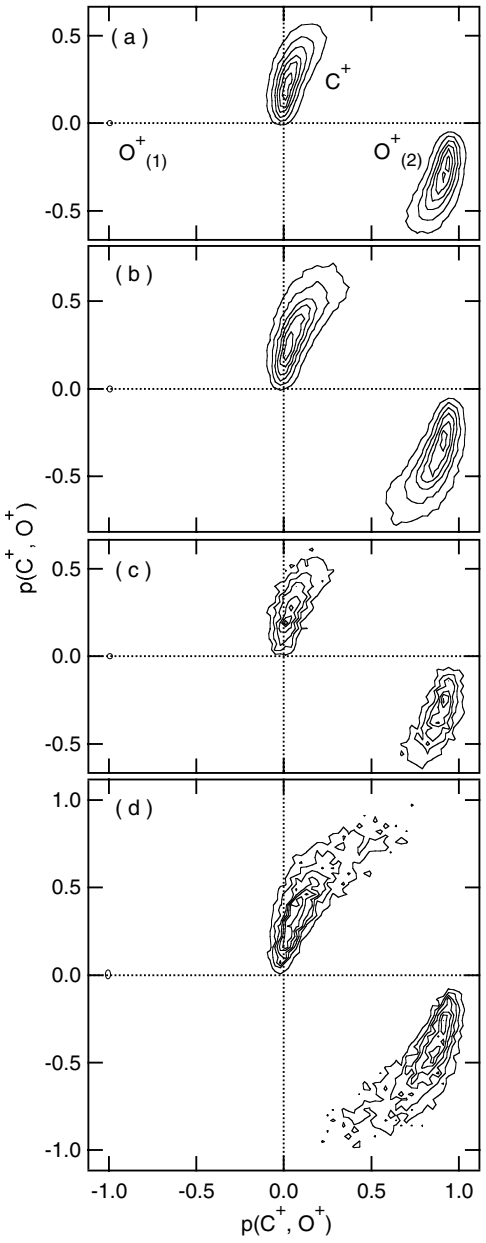

FIG. 2. Newton diagrams for the three-body breakup $CO_2^{3+} \rightarrow C^+ + O^+ + O^+$. (a) For the excitation at the O 1$s \rightarrow \sigma^*$ shape resonance (560 eV), (b) for the O 1$s \rightarrow 2\pi_u$ excitation (535.4 eV), (c) for the excitation to the state with the bending motion perpendicular to the E vector (i.e., B_1 in C_{2v}), by 535.4-eV photons, and (d) for the excitation to the state with the bending motion parallel to E (i.e., A_1 in C_{2v}), by 535.4-eV photons. The scale of contour plots is linear and relative.

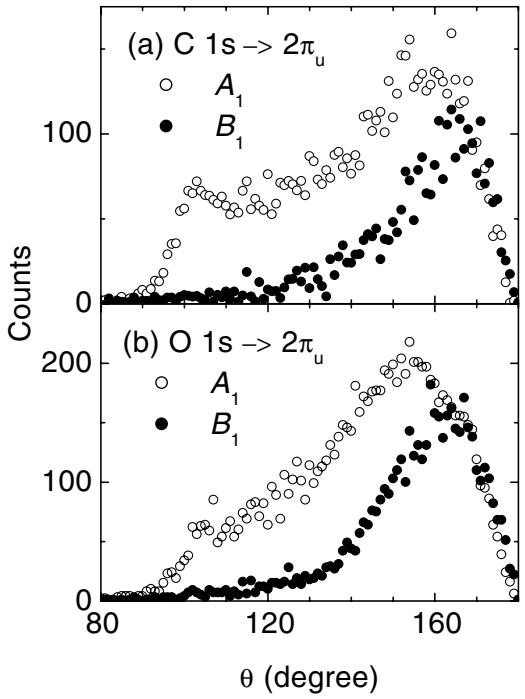

FIG. 3. The θ distributions, recorded for 4π-sr measurements, for the excitation to the state with the polarization direction parallel to the bending motion (A_1: open circle) and to the state with the polarization direction perpendicular to the bending motion (B_1: closed circle). Here θ is the O-O correlation angle between the linear momenta of the two O^+ ions obtained by the triple-ion-coincidence momentum imaging technique for the process $CO_2^{3+} \rightarrow C^+ + O^+ + O^+$. (a) C $1s^{-1}2\pi_u$ and (b) O $1s^{-1}2\pi_u$.

normalized vector is placed on the negative x axis. The linear momentum of C^+ is then plotted in the positive x and y direction, while the linear momentum of the second O^+ in the positive x and negative y directions. The intensity is given in the form of contour plots in linear scale. The data shown in Fig. 2 are recorded at SPring-8 and are practically the same as those recorded at Super-ACO.

As references for later discussion, we first show diagrams (a) and (b) recorded at the O $1s \rightarrow \sigma^*$ shape resonance at 560 eV (note that there are two shape resonances for O $1s$ ionization of CO_2, σ_g^* at 542 eV, and σ_u^* at 560 eV) and at the O $1s \rightarrow 2\pi_u$ excitation at 535.4 eV, respectively. Here the two RT pair states have not been separated yet. The C^+ ion goes off slightly transverse to the two O^+ ions on average even at the O $1s \rightarrow \sigma^*$ shape resonance, even though the molecule is believed to have a linear geometry before dissociation. Nearly the same result is obtained for the C $1s \rightarrow \sigma^*$ excitation. Even though the stable geometry is linear, the C atom goes off slightly transverse to the molecular axis due to zero-point bending vibration. The Coulomb explosion enhances this small displacement, resulting in a non-negligible linear momentum of the C^+ ion transverse the two O^+ ions. At the O $1s \rightarrow 2\pi_u$ excitation, we can clearly see the long tail for each island which illustrates that the C^+ ion goes off transverse to the two O^+ ions more than those at the O $1s \rightarrow \sigma^*$ shape resonance. Similar results are obtained for the C $1s \rightarrow 2\pi_u$ excitation. These findings support our postulation from the $(Z + 1)$ model that the O $1s^{-1}2\pi_u$ state is bent whereas the O $1s^{-1}\sigma^*$ and ionic O $1s^{-1}$ states are basically linear.

We now show our key results, diagrams (c) and (d) in Fig. 2. In both diagrams, the excitation energy is set at the O $1s \rightarrow 2\pi_u$ excitation peak. In the construction of diagram (c), however, we selected the events in which the vector product of the two linear momenta of the two O^+ ions, $p(O^+_{(1)}) \times p(O^+_{(2)})$, is parallel to E, with the angles between $p(O^+_{(1)}) \times p(O^+_{(2)})$ and E smaller than 20°. In this way we selected the state in which the direction of the bending motion is perpendicular to E, i.e., the B_1 state in the bent geometry of C_{2v} symmetry (see Fig. 1). In constructing diagram (d), on the other hand, we selected the events in which $p(C^+)$ is parallel to E, with the angles between $p(C^+)$ and E smaller than 20°. In this way we selected the state in which the direction of the bending motion is parallel to E, i.e., the A_1 state in the bent geometry of C_{2v} symmetry (see Fig. 1). The purities of the A_1 and B_1 states thus selected are estimated to be better than 96%.

Diagram (c) coincides with diagram (a) and illustrates that the displacement of the C atom due to the bending motion does not occur significantly in the direction perpendicular to E. In other words, the B_1 state thus probed has a linear geometry. In diagram (d), we can clearly see that the very long tail appears for each island, illustrating that the C^+ ion goes off significantly transverse to the two O^+ ions. The equivalent results are obtained for the C $1s \rightarrow 2\pi_u$ excitation. This is a direct proof that the bending motion proceeds significantly in the A_1 state. A highly excited bending motion in a linear state with A_1 symmetry, which might cause a tail structure, cannot be excited from the linear ground state due to Franck-Condon principle. The initial vibrational wave packet has little momentum. The force to push the C atom at right angles relative to the molecular axis must come with time from the electronic potential energy surface. Thus the state with A_1 symmetry probed here must have a stable bent geometry.

We now focus on the O-O correlation angle θ between the two linear momenta of the two O^+ ions detected in coincidence with C^+. We plot in Figs. 3(a) and 3(b) the signal counts as a function of θ (hereafter referred to as θ distribution) for the excitation to C $1s^{-1}2\pi_u$ A_1 and B_1 and O $1s^{-1}2\pi_u$ A_1 and B_1, respectively. The data shown in Fig. 3 are recorded at SPring-8 and are practically the same as those recorded at Super-ACO. The θ distributions in Fig. 3 are obtained from the measurements for all solid angles 4π sr and plotted for unit angle $d\theta$, integrated over the azimuth angle ϕ. To extract the relative flux per unit solid angle $d\Omega = d\phi\, d\theta \sin\theta$ from the θ distribution of Fig. 3 one should divide the signal counts of Fig. 3 by $2\pi \sin\theta$.

It has been found that the θ distributions for C $1s^{-1}2\pi_u\ B_1$ and O $1s^{-1}2\pi_u\ B_1$ coincide with one another and also with those for C $1s^{-1}\sigma^*$ and O $1s^{-1}\sigma^*$ (not shown here), exhibiting a peak at $\sim 165°$. The θ distributions peaking at $\sim 165°$ reflect the dissociation geometry starting at the Condon point where the excitation takes place from the linear ground state with a zero-point distribution.

The θ distributions for C $1s^{-1}2\pi_u\ A_1$ and O $1s^{-1}2\pi_u\ A_1$, on the other hand, exhibit a peak at $\sim 155°$ and extend to lower angles, forming a second peak at $\sim 100°$. These two characteristic angles are nearly the same for C $1s^{-1}2\pi_u\ A_1$ and O $1s^{-1}2\pi_u\ A_1$; only the distributions between these two angles are different. According to the Franck-Condon principle, the molecule is still linear immediately after excitation. Then the molecule starts to bend towards the turning point of the bending motion. The major peak at $\sim 155°$ reflects the dissociation geometry after the Auger decay near the Condon point where the excitation takes place. The long tail which extends to $\sim 100°$ on the other hand reflects the dissociation geometry after the Auger decay which occurs on the way to the turning point in the core-excited states. The lifetime of the C (O) $1s^{-1}$ state is ~ 7 (3) fs whereas the period of the bending vibration is ~ 46 fs: hence only a small fraction ($\leq 4\%$) of the excited molecules can reach the turning point before the Auger decay takes place.

Care should be taken in interpreting the angle $\sim 100°$ where the θ distribution drops to zero. At first glance one might think that this angle corresponds solely to the turning point. A simple Coulomb explosion model, on the other hand, suggests that one cannot detect the two O^+ ions with θ smaller than $\sim 120°$ because of the Coulomb repulsion between the two O^+ ions. The distribution of the θ smaller than $\sim 120°$ can be explained by taking account of the kinetic energy given to the O atom in the evolution of the bending motion in the core-excited state and of unequal charge distributions for the three ions at the early stage of the dissociation after the Auger decay. We cannot draw a decisive conclusion on whether the observed cutoff angle of $\sim 100°$ corresponds predominantly to the turning point in the core-excited state (initial-state effect) or to the cut-off angle in the Coulomb explosion (final-state effect).

In conclusion, using the triple-ion-coincidence momentum imaging technique and focusing on the dependence of the measured quantities on the polarization of the incident light, we have probed, directly and separately, the linear and bent geometries for the B_1 and A_1 Renner-Teller pair states, as a direct proof of the static Renner-Teller effect. We believe that the new technique discussed here will open a new field, i.e., a direct probe of changing geometry for each molecular excited state, even for overlapping states with different symmetries.

The SPring-8 experiment was carried out with the approval of the SPring-8 program advisory committee (Proposal No. 2000A0201-NS-np) and supported in part by a Grants-in-Aid for Scientific Research from the Japan Society of the Promotion of Science and by the Matsuo Foundation. The authors are grateful to the staff of SPring-8 and LURE for their help during the course of the experiments.

*Corresponding author: ueda@tagen.tohoku.ac.jp

[1] M. Neeb, J. E. Rubensson, M. Biermann, and W. Eberhardt, J. Electron Spectrosc. Relat. Phenom. **67**, 261 (1994).
[2] O. Björneholm *et al.,* Phys. Rev. Lett. **79**, 3150 (1997), and references cited therein.
[3] T. Lebrun, M. Lavollee, M. Simon, and P. Morin, J. Chem. Phys. **98**, 2534 (1993).
[4] M. Simon *et al.,* Chem. Phys. Lett. **238**, 42 (1995).
[5] J. Adachi, N. Kosugi, E. Shigemasa, and A. Yagishita, J. Chem. Phys. **102**, 7369 (1995).
[6] K. Ueda *et al.,* Phys. Rev. Lett. **83**, 3800 (1999).
[7] P. Morin *et al.,* Phys. Rev. A **61**, 050701 (2000).
[8] G. R. Wight and C. E. Brion, J. Electron Spectrosc. Relat. Phenom. **3**, 191 (1973).
[9] J. D. Bozek, N. Saito, and I. H. Suzuki, Phys. Rev. A **51**, 4563 (1995).
[10] J. Adachi, N. Kosugi, E. Shigemasa, and A. Yagishita, J. Chem. Phys. **107**, 4919 (1997).
[11] E. Kukk, J. D. Bozek, and N. Berrah, Phys. Rev. A **62**, 032708 (2000).
[12] H. Köppel, W. Domcke, and L. S. Cederbaum, Adv. Chem. Phys. **57**, 59 (1984).
[13] I. B. Bersuker and V. Z. Polinger, *Vibronic Interactions in Molecules and Crystals* (Springer, Berlin, 1989).
[14] S. Tanaka and Y. Kayanuma, Solid State Commun. **100**, 77 (1996).
[15] S. Tanaka, Y. Kayanuma, and K. Ueda, Phys. Rev. A **57**, 3437 (1998).
[16] S. I. Itoh, S. Tanaka, and Y. Kayanuma, Phys. Rev. A **60**, 4488 (1999).
[17] K. Ueda *et al.,* Phys. Rev. Lett. **85**, 3129 (2000).
[18] See, for example, G. Herzberg, *Infrared and Raman Spectra of Polyatomic Molecules* (Van Nostrand, New York, 1973).
[19] N. Saito *et al.,* Phys. Rev. A **62**, 042503 (2000).
[20] Y. Muramatsu *et al.,* Chem. Phys. Lett. **330**, 91 (2000).
[21] R. N. Zare, Mol. Photochem. **4**, 1 (1972).
[22] G. E. Busch and K. R. Wilson, J. Chem. Phys. **56**, 3638 (1972).
[23] H. Ohashi *et al.,* Nucl. Instrum. Methods Phys. Res., Sect. A **467–468**, 533 (2001).
[24] M. Lavollée, Rev. Sci. Instrum. **70**, 2968 (1999).